Recent developments in ab initio studies of nuclear matter

Kai Hebeler

Mainz, August 27, 2026

SFB 1245

TECHNISCHE
UNIVERSITÄT
DARMSTADT

Outline

1. Inner crust and outer core: phase structure and EOS

2. Liquid-gas transition and EOS at finite temperature

3. Inner and outer core: extension to hypermatter

MBPT calculations of dense matter (here T=0) based on chiral EFT interaction

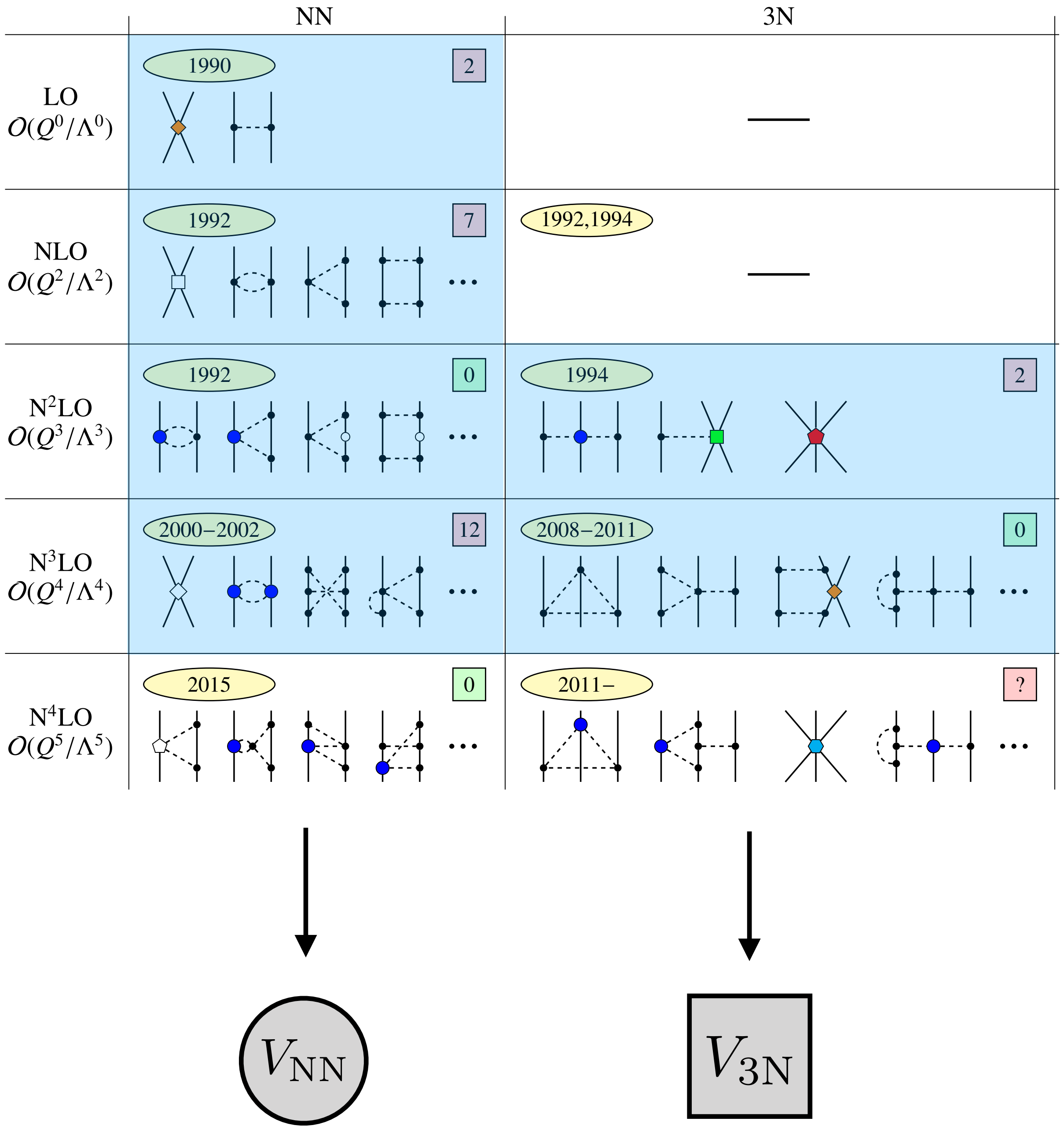

$$\langle 1'2'|V_{NN}|12\rangle = \langle \mathbf{k}_1'\sigma_1'\tau_1'\mathbf{k}_2'\sigma_2'\tau_2'|V_{NN}|\mathbf{k}_1\sigma_1\tau_1\mathbf{k}_2\sigma_2\tau_2\rangle\,,$$
$$\langle 1'2'3'|V_{3N}|123\rangle = \langle \mathbf{k}_1'\sigma_1'\tau_1'\mathbf{k}_2'\sigma_2'\tau_2'\mathbf{k}_3'\sigma_3'\tau_3'|V_{3N}|\mathbf{k}_1\sigma_1\tau_1\mathbf{k}_2\sigma_2\tau_2\mathbf{k}_3\sigma_3\tau_3\rangle$$

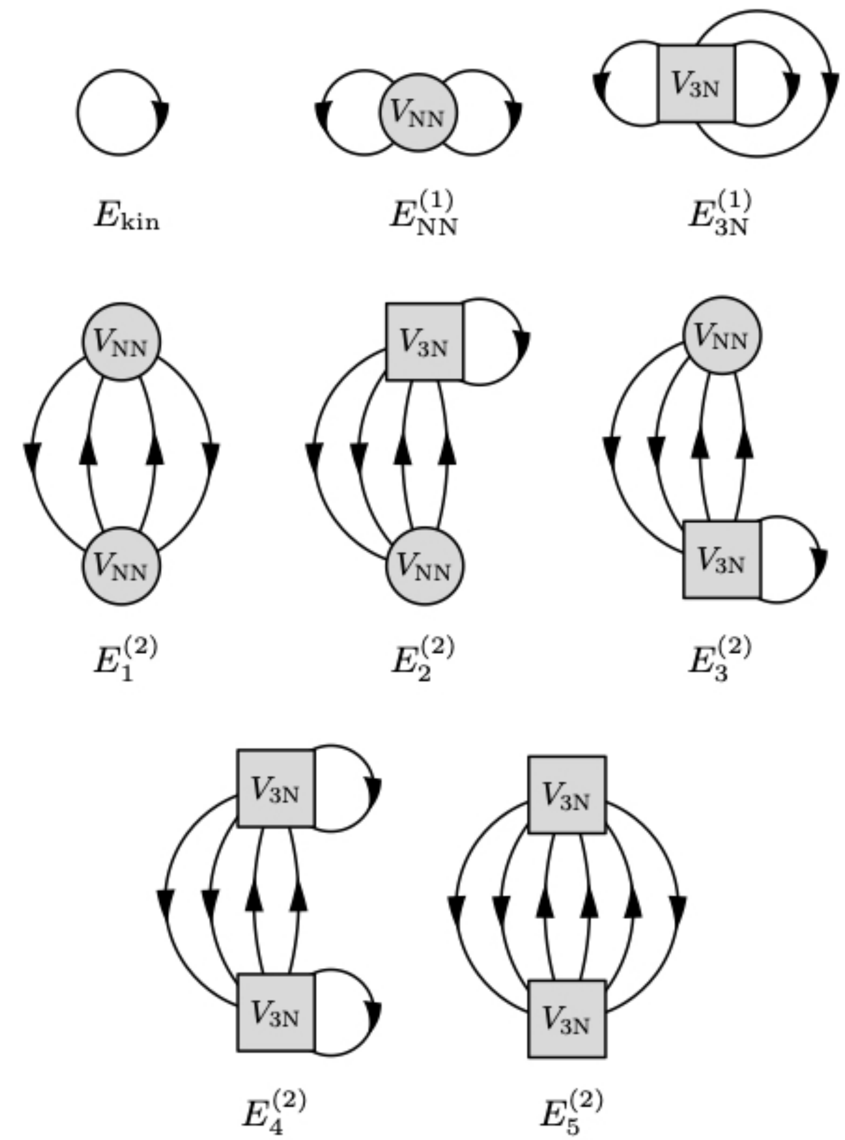

+ …

talk by Yannick Dietz:
Details on current developments on these MBPT calculations

MBPT framework - Illustration: Second-order diagram

$$E^{(2)}_{\mathrm{NN+3N,eff}} = \frac{1}{4}\left[\prod_{i=1}^{4} \mathrm{Tr}_{\sigma_i} \int \frac{d\mathbf{k}_i}{(2\pi)^3}\right] \left|\langle 12|V^{(2)}_{\mathrm{as}}|34\rangle\right|^2$$
$$\times \frac{n_{\mathbf{k}_1} n_{\mathbf{k}_2}(1-n_{\mathbf{k}_3})(1-n_{\mathbf{k}_4})}{\varepsilon_{\mathbf{k}_1}+\varepsilon_{\mathbf{k}_2}-\varepsilon_{\mathbf{k}_3}-\varepsilon_{\mathbf{k}_4}}(2\pi)^3$$
$$\times \delta(\mathbf{k}_1+\mathbf{k}_2-\mathbf{k}_3-\mathbf{k}_4).$$

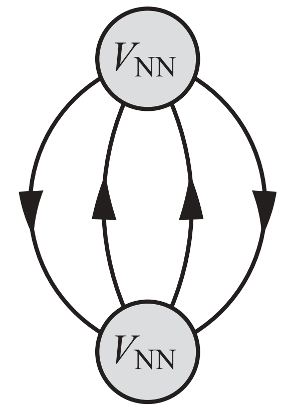

Partial wave representation:

$$\sum_{S,M_S,M'_S} \left|\langle \mathbf{k} S M_S | V^{(2)}_{\mathrm{as}} | \mathbf{k}' S M'_S\rangle\right|^2$$
$$= \sum_L P_L(\cos\theta_{\mathbf{k},\mathbf{k}'}) \sum_{J,l,l',S} \sum_{\tilde{J},\tilde{l},\tilde{l}'} (4\pi)^2 i^{(l-l'+\tilde{l}-\tilde{l}')}(-1)^{\tilde{l}+l'+L}$$
$$\times \mathcal{C}^{L0}_{l0\tilde{l}0}\mathcal{C}^{L0}_{l'0\tilde{l}'0}\sqrt{(2l+1)(2l'+1)(2\tilde{l}+1)(2\tilde{l}'+1)}$$
$$\times (2J+1)(2\tilde{J}+1)\begin{Bmatrix} l & S & J \\ \tilde{J} & L & \tilde{l}' \end{Bmatrix}\begin{Bmatrix} J & S & l' \\ \tilde{l} & L & \tilde{J} \end{Bmatrix}$$
$$\times \langle k|V^{(2)}_{Sl'lJ}|k'\rangle\langle k'|V^{(2)}_{S\tilde{l}'\tilde{l}\tilde{J}}|k\rangle[1-(-1)^{l+S+1}]$$
$$\times [1-(-1)^{\tilde{l}+S+1}],$$

e.g., KH, Schwenk PRC 82, 014314 (2013)

- hard to automatize and generalize to higher order diagrams
- prone to mistakes

Single-particle vector representation:

$$\frac{E^{(2)}_{\mathrm{NN}}}{V} = +\frac{1}{4}\sum_{\substack{ij\\ab}} \frac{\langle ij|\mathscr{A}_{12}V_{\mathrm{NN}}|ab\rangle\,\langle ab|\mathscr{A}_{12}V_{\mathrm{NN}}|ij\rangle}{D_{ijab}}$$

- each diagram just a one line or few lines of code
- straightforward to automatize via code generation
- adaptive evaluation of integrals using Monte-Carlo techniques
- allows inclusion of 3N contributions without normal ordering

Matter at finite temperature and general proton fractions

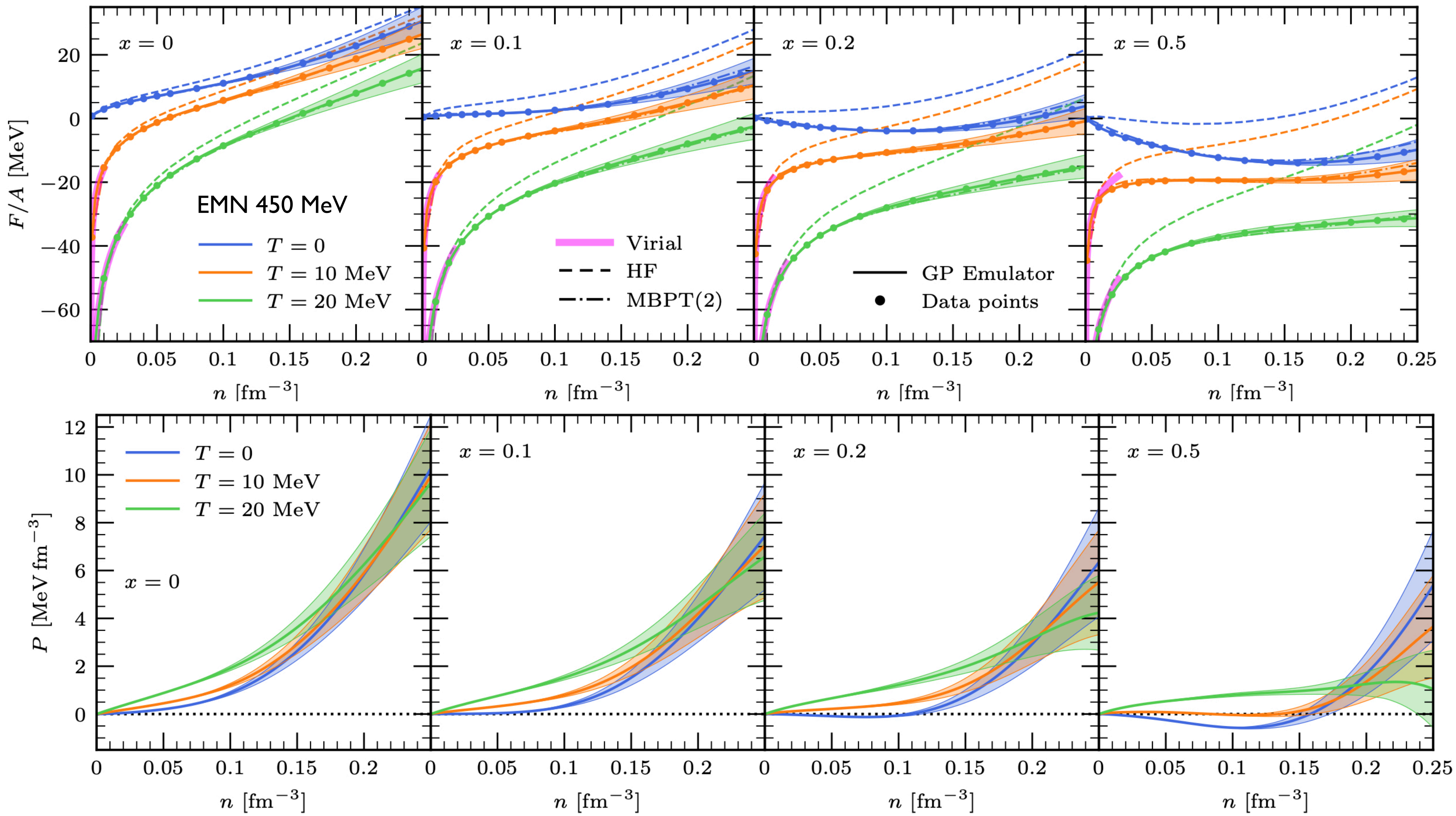

Jonas Keller

Keller, KH, Schwenk, PRL 130, 072701 (2023)

- evaluation of grand canonical potential at finite T in MBPT up to third order:

$$\Omega\left(T, \mu_n, \mu_p\right) = -\frac{1}{\beta} \ln \mathrm{Tr}\left(e^{-\beta\left(H - \mu_n N_n - \mu_p N_p\right)}\right)$$

- implementation of Gaussian process emulator for efficient interpolation and evaluation of thermodynamic quantities

Neutron star matter and thermal pressure

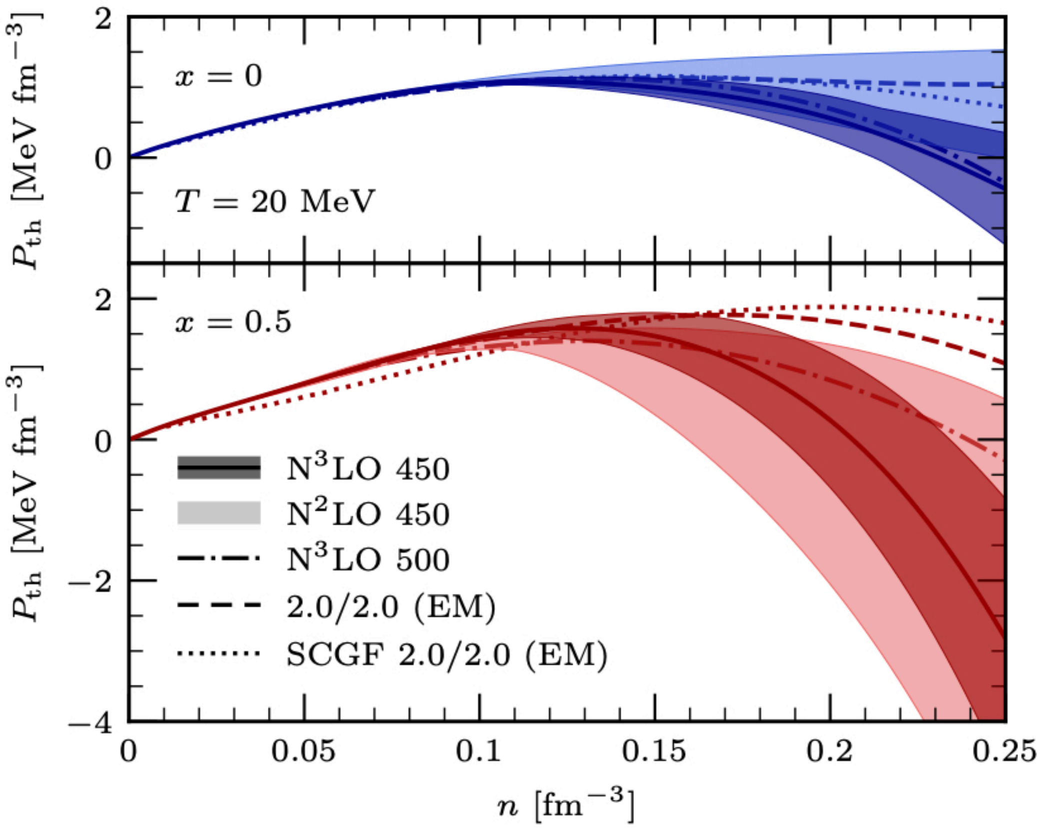

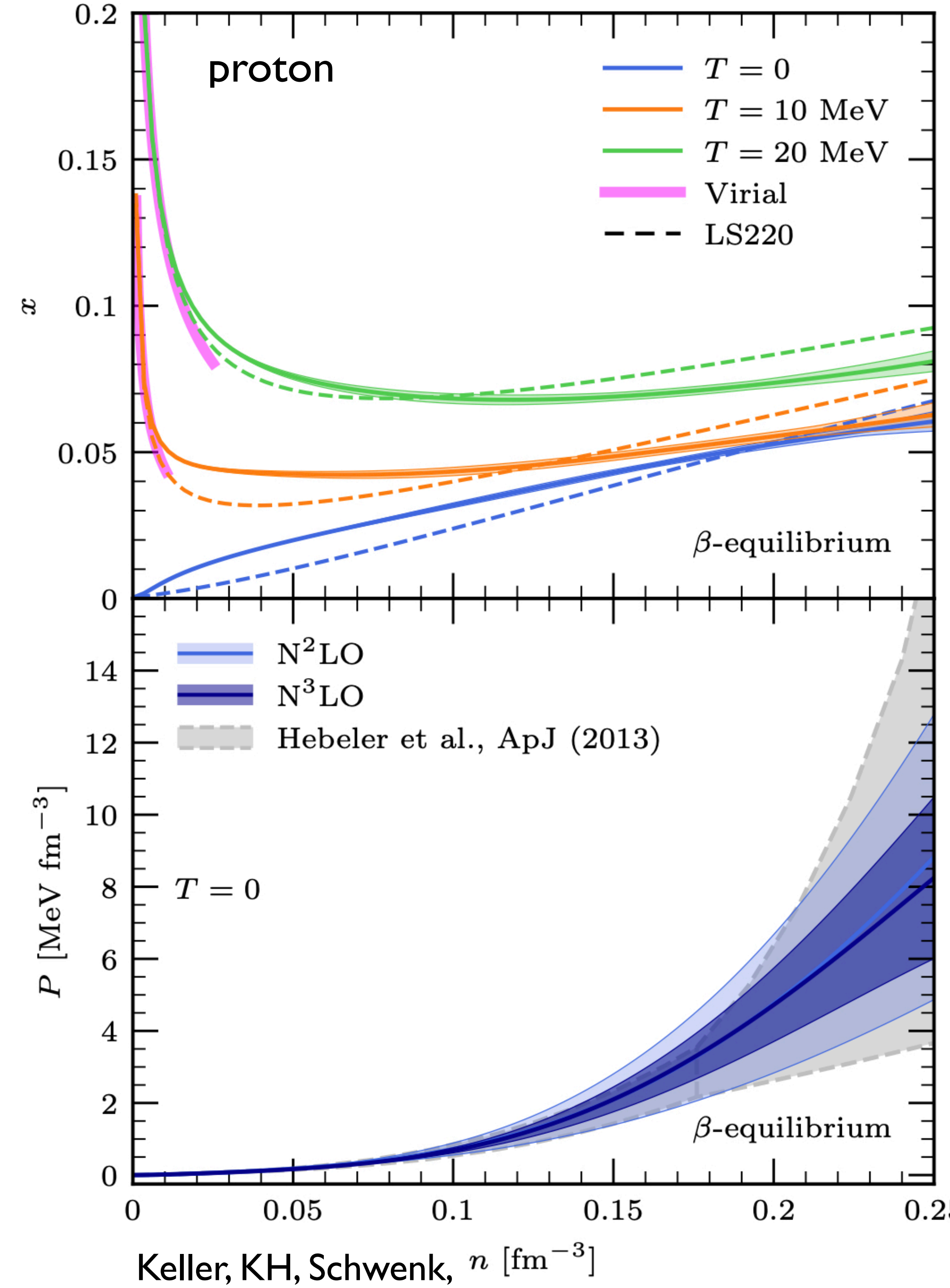

Keller, KH, Schwenk, PRL 130, 072701

- incorporation of beta equilibrium

$$m_n + \mu_n = (m_p + \mu_p) + (m_e + \mu_e)$$

- reduced interaction uncertainties compared to previous calculations at N^{2}LO
- $P_{\rm th}(T) = P(T) - P(T=0)$ becomes negative at higher densities due to contributions from 3N interactions

Phase coexistence of nuclear matter (T=0)

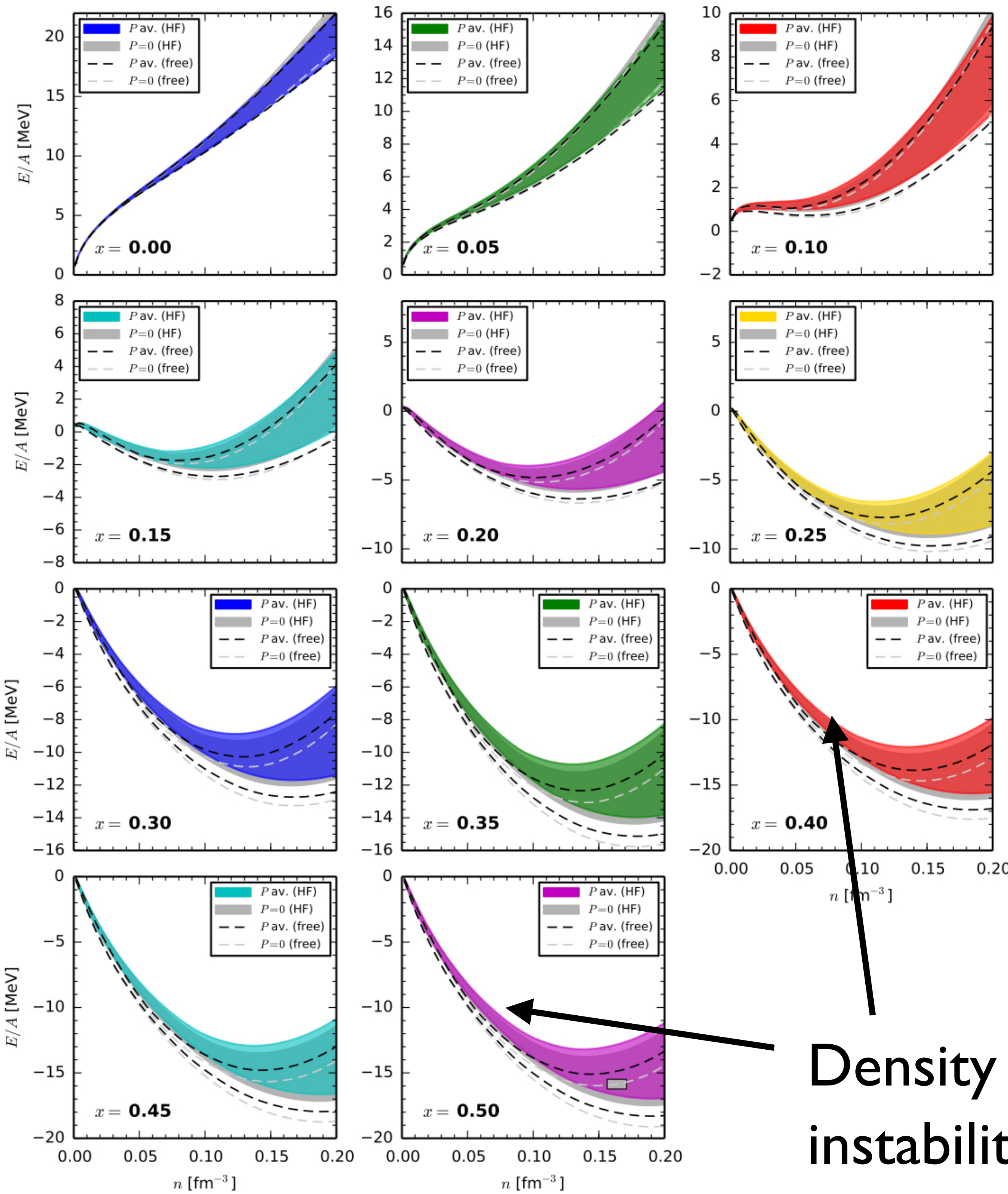

Drischler, KH, Schwenk
PRC 93, 0054314 (2015)

proton fraction:

$$x = \frac{n_p}{n} = \frac{n_p}{n_p + n_n}$$

pressure:

$$P(n) = n^2 \frac{\partial(E/A)}{\partial n}\Big|_x$$

chemical potentials:

$$\mu_\tau = \frac{\partial(E/A \cdot n)}{\partial n_\tau}$$

Density regions with negative pressure signal instability of homogeneous phase (spinodal region ⟶ phase coexistence)

Phase coexistence of nuclear matter (T=0)

For coexistence of two phases, 1 and 2, the following conditions must hold:

$$P^{(1)} = P^{(2)}, \ \mu_n^{(1)} \geq \mu_n^{(2)}, \ \mu_p^{(1)} \geq \mu_p^{(2)}$$

(**phase 2** is assumed to be the high-density phase)

Luis Hoff

Different possible scenarios:

1. $n_n^{(1)} = 0, n_p^{(1)} = 0, \ P^{(1)} = P^{(2)} = 0$

   coexistence with vacuum

2. $n_n^{(1)} > 0, \ \mu_n^{(1)} = \mu_n^{(2)}, \ n_p^{(1)} = 0$

   coexistence with neutron matter, "neutron drip"

3. $n_n^{(1)} > 0, \ \mu_n^{(1)} = \mu_n^{(2)}$

   $n_p^{(1)} > 0, \ \mu_p^{(1)} = \mu_p^{(2)}$

   coexistence with nuclear matter, "proton drip"

Keller, KH, Pethick, Schwenk, PRL 132, 232701 (2024)

Luis Hoff, Master Thesis (2026), Göttling, Hoff, HF, Schwenk, PRC 113, 055804 (2026)

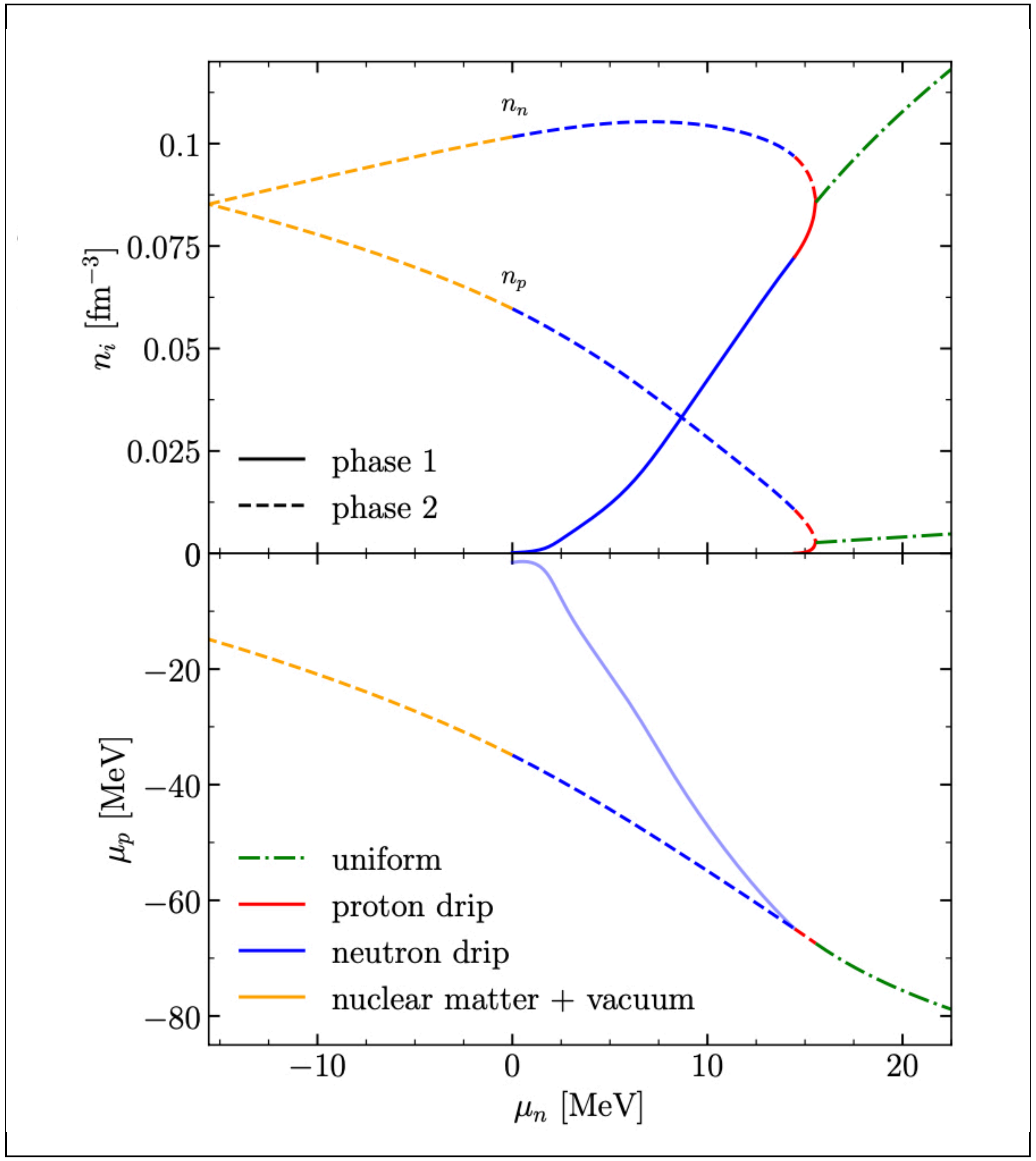

Phase diagram of nuclear matter (T=0)

coexistence of dripped neutron/protons occurs along lines in the (n_n, n_p) or $(n = n_n + n_p, x = n_p/n)$ plane with:

$$n_{\rm n} = n_{\rm n}^{(1)}(1-u) + n_{\rm n}^{(2)}u$$
$$n_{\rm p} = n_{\rm p}^{(1)}(1-u) + n_{\rm p}^{(2)}u$$

with the volume fraction $u \in [0,1]$

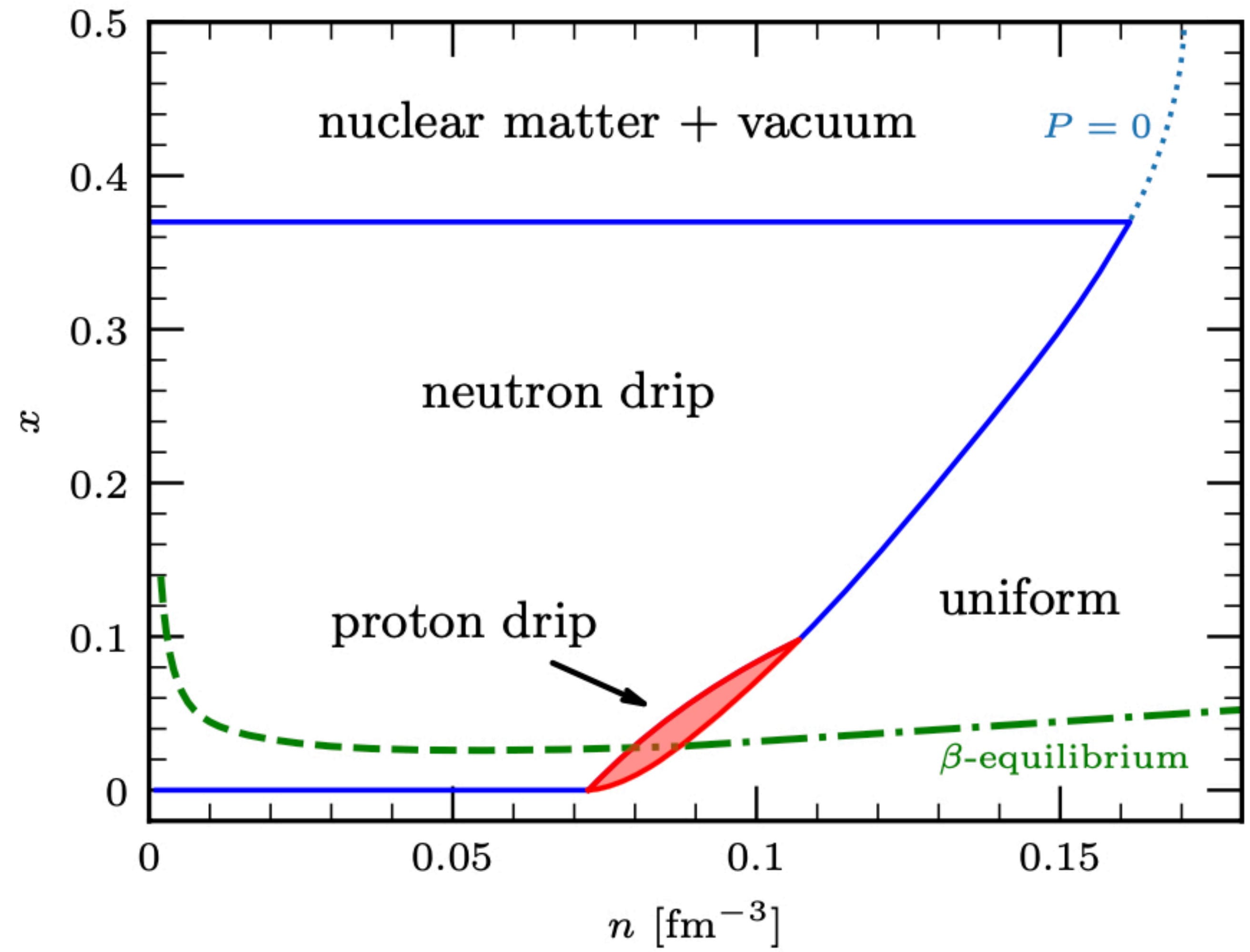

Keller, KH, Pethick, Schwenk, PRL 132, 232701 (2024)

- neutron drop is possible for large region of phase diagram
- proton drop only in a restricted region, overlaps with EOS in beta equilibrium

Construction of crust EOS based on chiral interactions

- for study of phase diagram, only bulk energy contributions are considered
- for calculation of equation of state, additional contributions like Coulomb and surface energy corrections need to be incorporated
- For neutron drip region:

Göttling, Hoff, HF, Schwenk, PRC 113, 055804 (2026)

Phase 1 (low-density PNM)

$$\left(\frac{E}{A}\right)^{(1)}(n,x) = \frac{E^{\text{bulk}}}{A}(n_n,0)$$

Phase 2 (high density)

$$\left(\frac{E}{A}\right)^{(2)}(n,x) = \frac{E^{\text{bulk}}}{A}(n,x) + \frac{E^{\text{C}}}{A}(n,x) + \frac{E^{\text{S}}}{A}(n,x)$$

- ✦ Assume spherical Wigner-Seitz cell containing PNM (phase 1)
- ✦ in center of cell nuclear matter is located (phase 2) with given proton fraction
- ✦ densities assumed to be uniform in both phases
- ✦ in addition the cell contains uniform electron gas

Luis Hoff

Construction of crust EOS based on chiral interactions

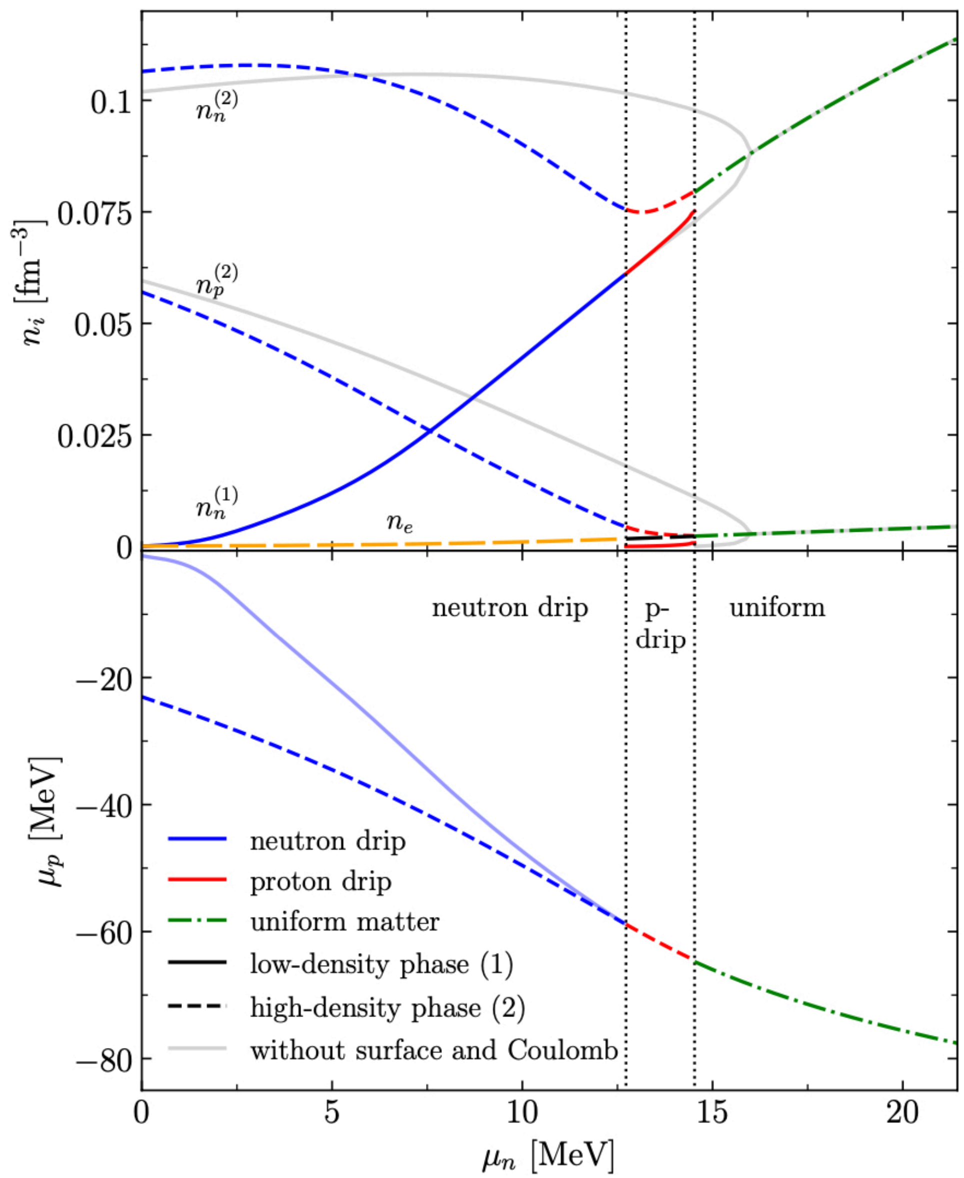

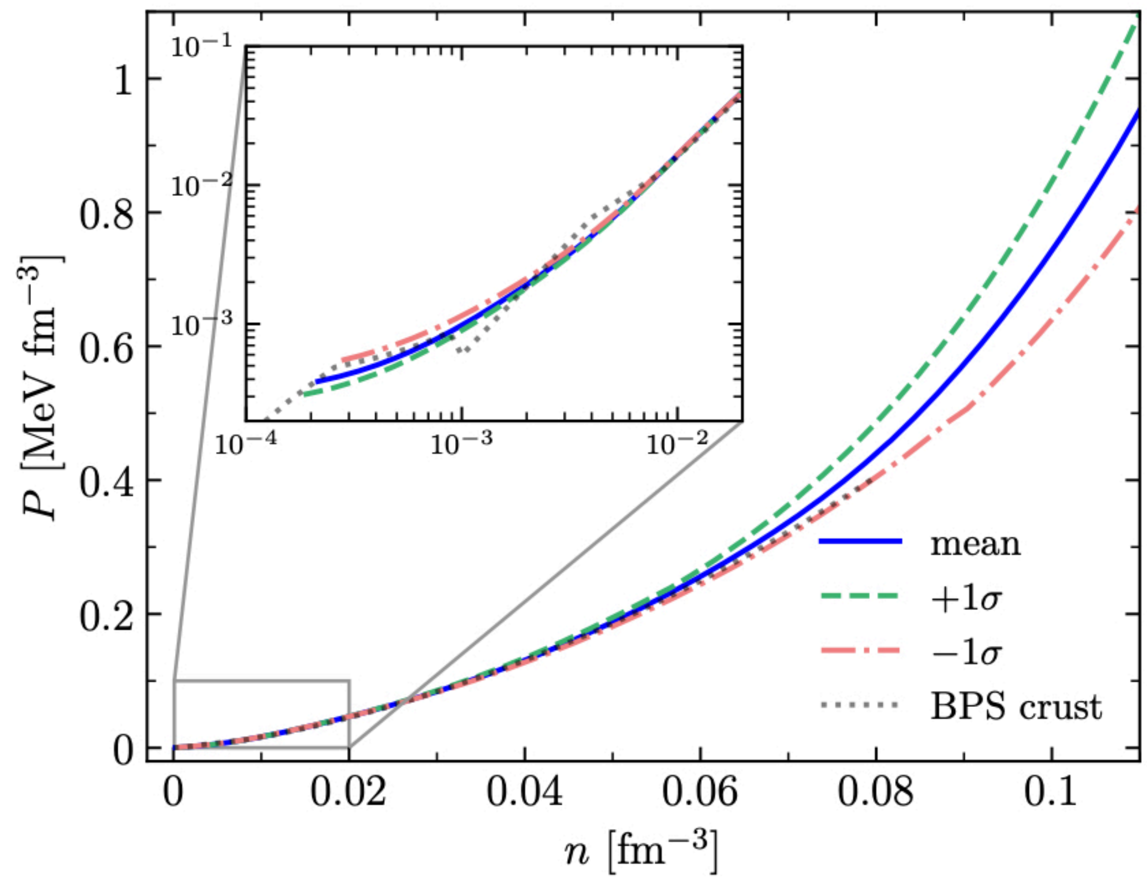

Göttling, Hoff, KH, Schwenk,
PRC 113, 055804 (2026)

Hannah Göttling

- Neutron- and proton drip regions remain after inclusion of corrections
- Moderate changes of densities and chemical potentials in both phases
- Good agreement with BPS crust EOS up to $n_0/2$

Critical temperature of symmetric matter

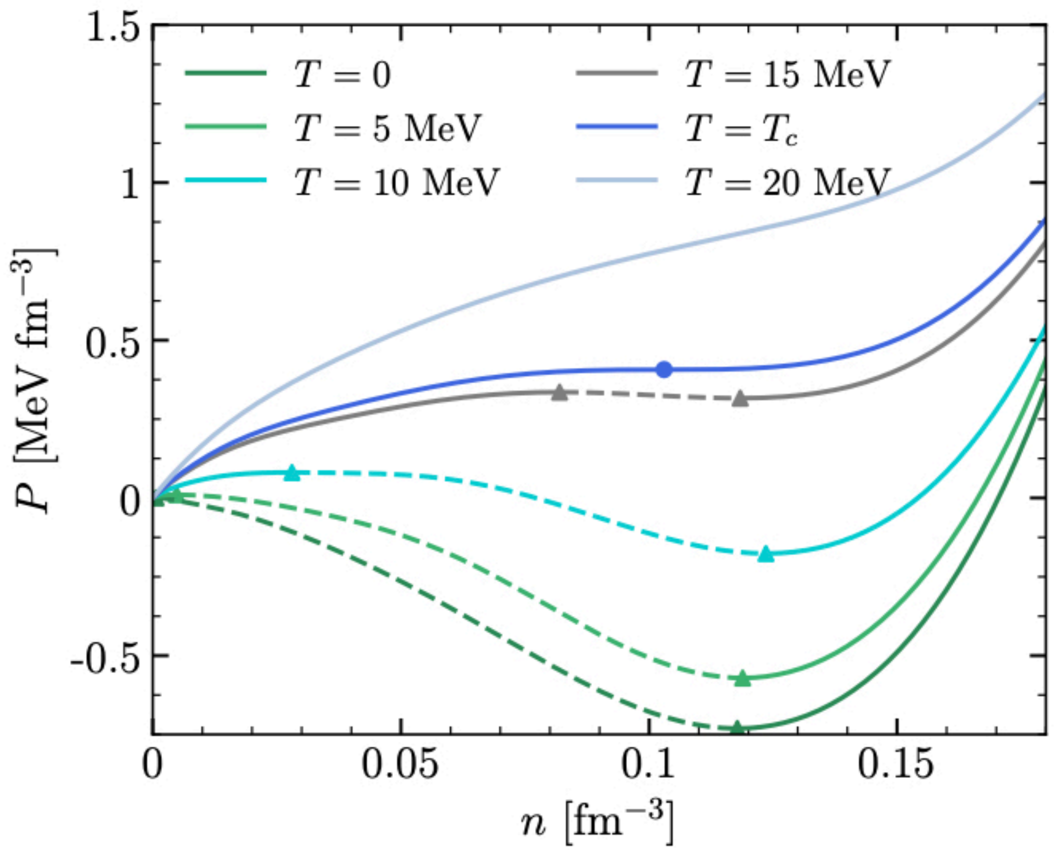

Maxwell construction in symmetric matter:

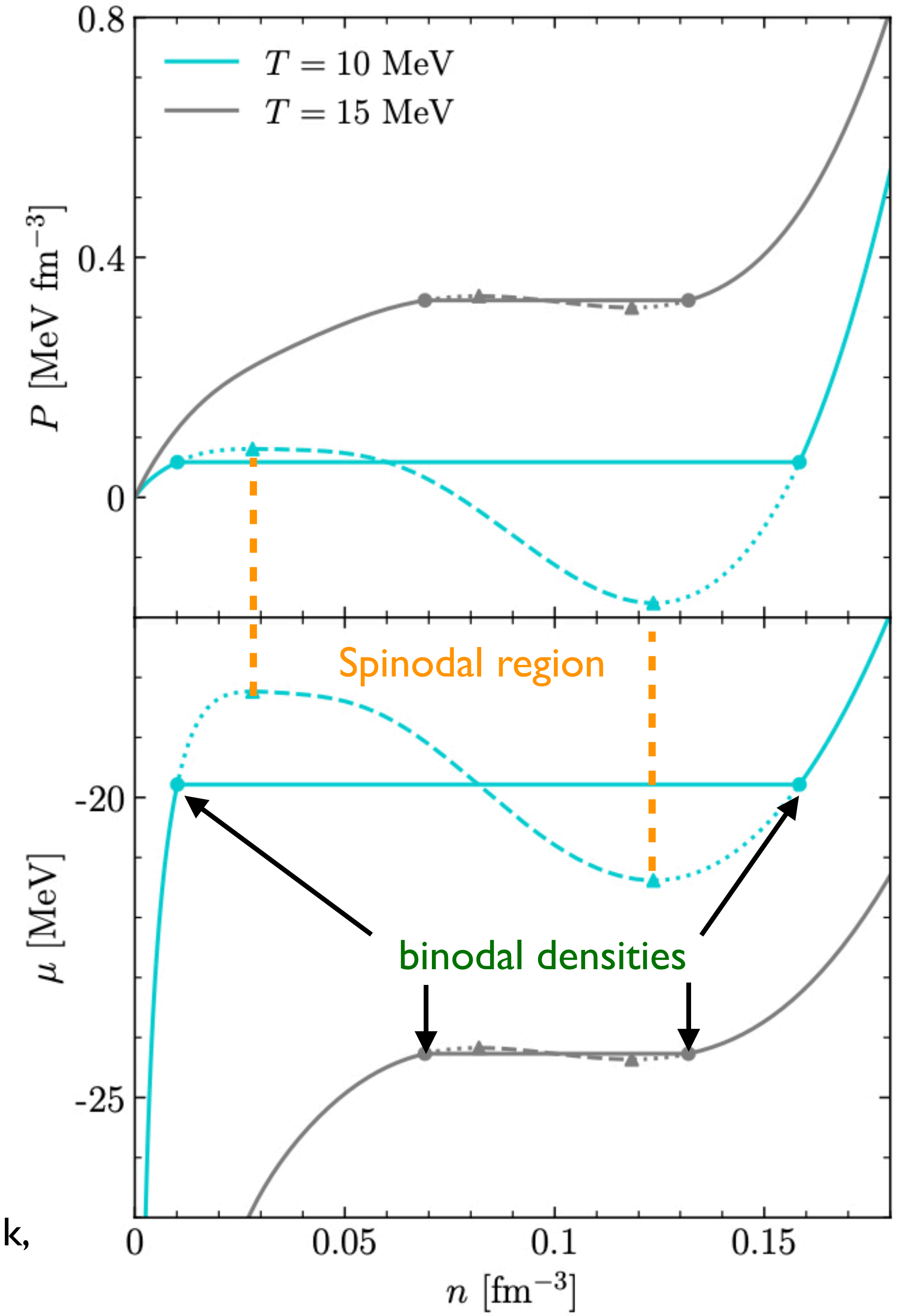

Göttling, Hoff, KH, Schwenk,
in preparation

Critical temperature of symmetric matter

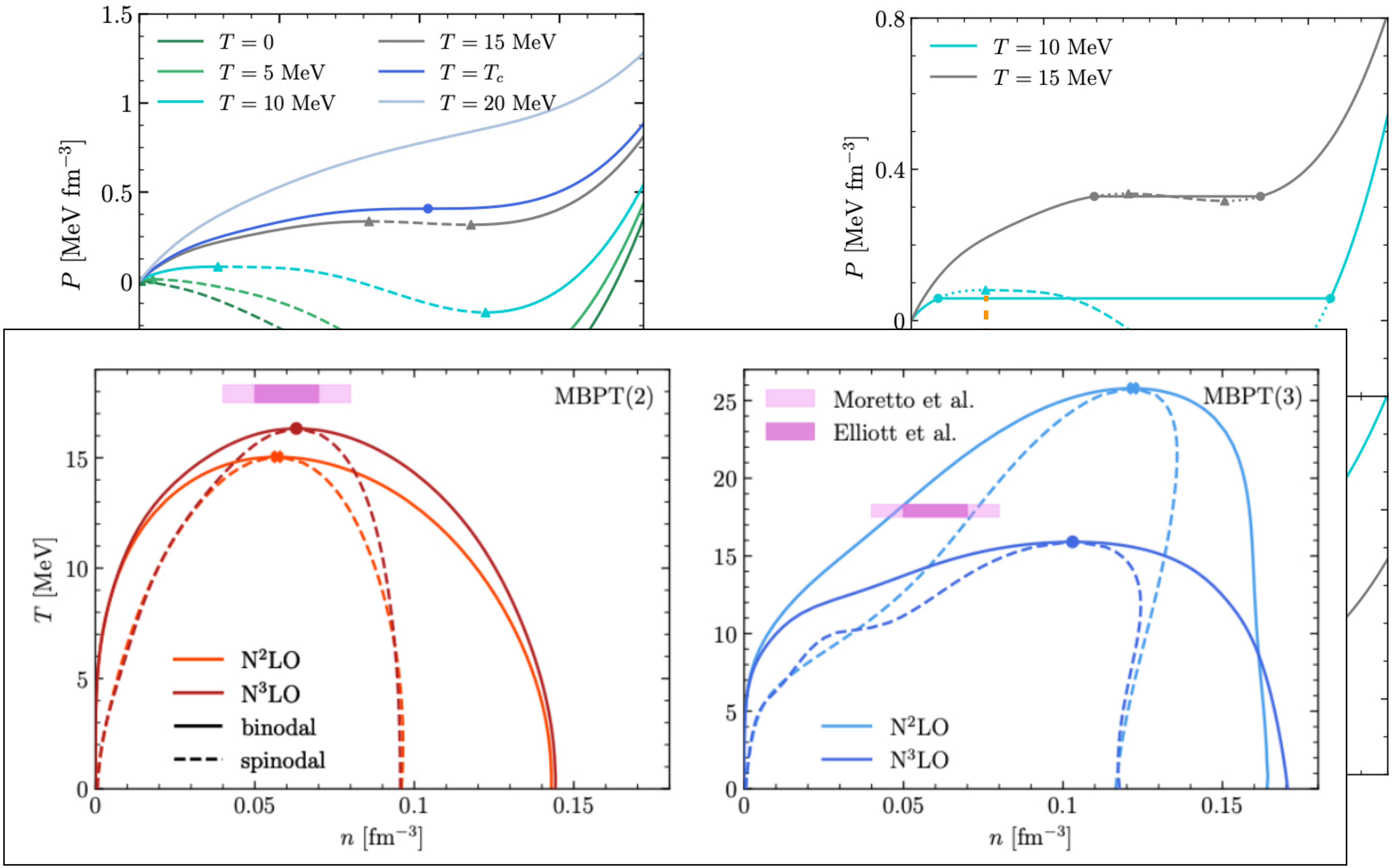

- large sensitivity of T_c to details of many-body calculations order in MBPT

Critical temperature of asymmetric matter

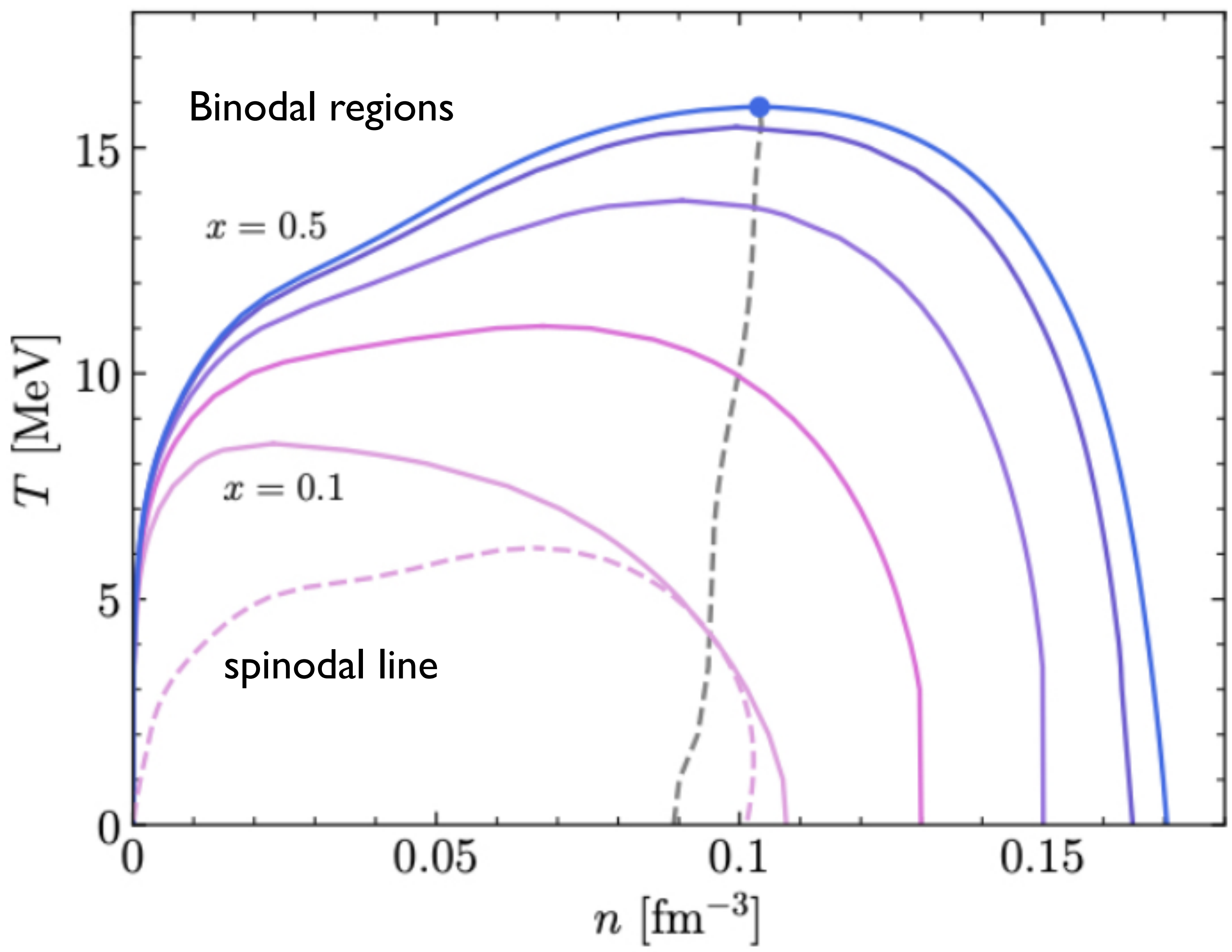

Göttling, Hoff, KH, Schwenk, in preparation

- critical density rather insensitive of proton fraction
- critical temperature decreasing with decreasing proton fraction

The “hyperon puzzle”

- Inclusion of hyperons can lead to a significant softening of EOS
- Incompatible to observed heavy neutron stars
- However, degree of softening sensitively depends on details of interactions

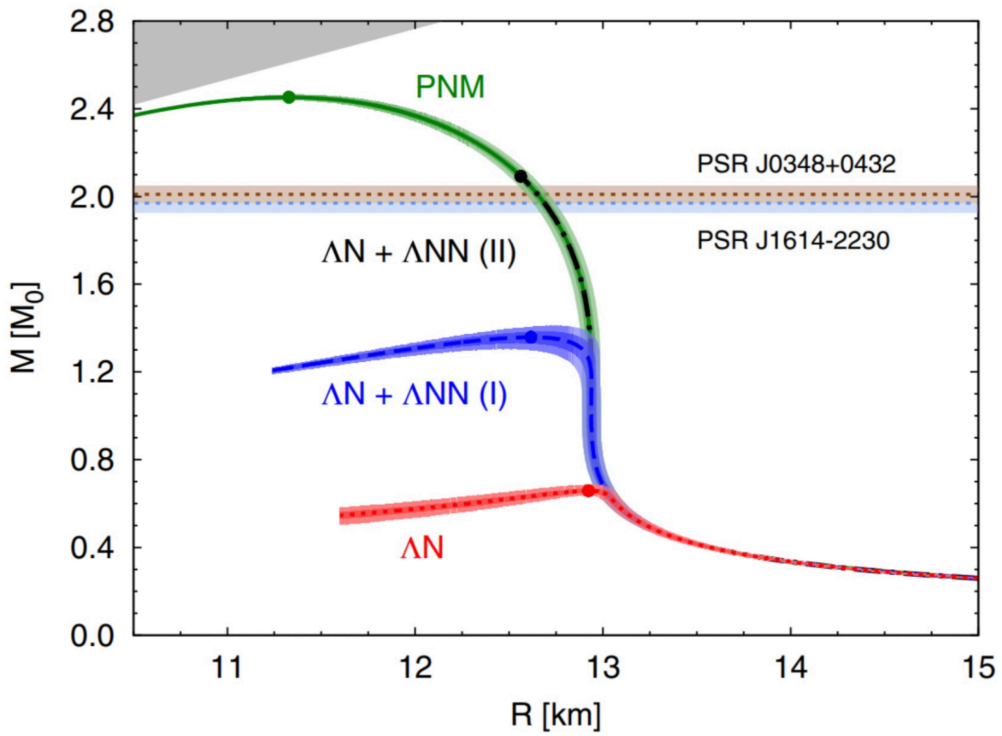

Lonardoni et al. PRL 114 (2015)

Hypermatter:
Inclusion of YN and YNN interactions

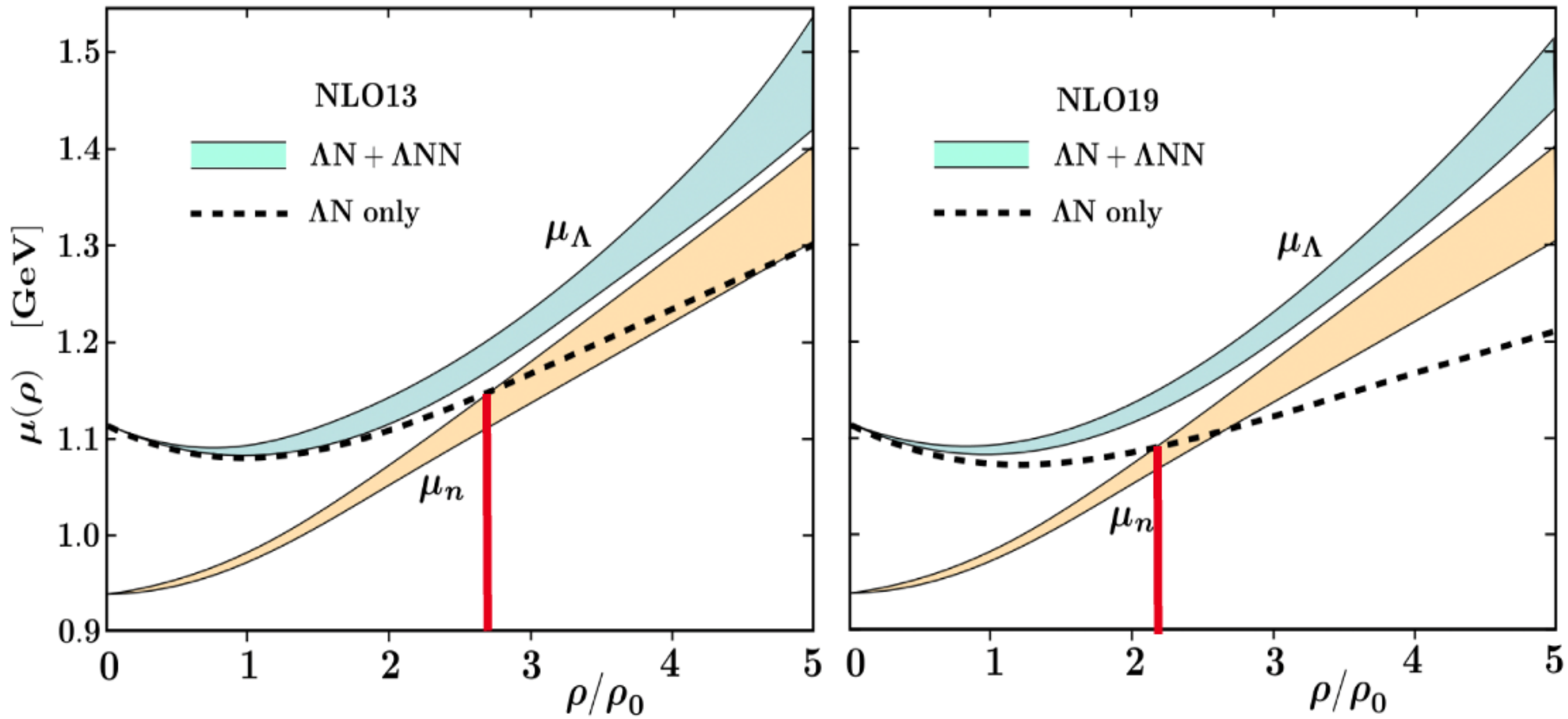

Gerstung et al. EPJA 56 (2020)

Samet Dokur

- Onset of hyperons in dense matter is determined by the chemical potential of nucleons and hyperons
- Goal: systematic study of hypermatter including uncertainties based on chiral EFT YN and YNN interactions

Hypermatter: Inclusion of YN and YNN interactions

particle	quarks	charge	Rest Mass (MeV^2)
Λ^0	uds	0	1115.68
Σ^+	uus	$+1$	1189.37
Σ^0	uds	0	1192.64
Σ^-	dds	-1	1197.45
Ξ^0	uss	0	1314.86
Ξ^-	dss	-1	1321.71
Ω^-	sss	-1	1672.45

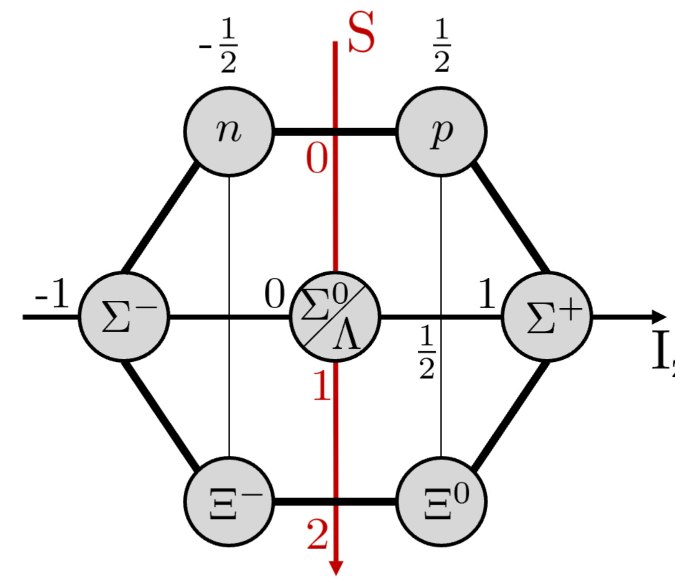

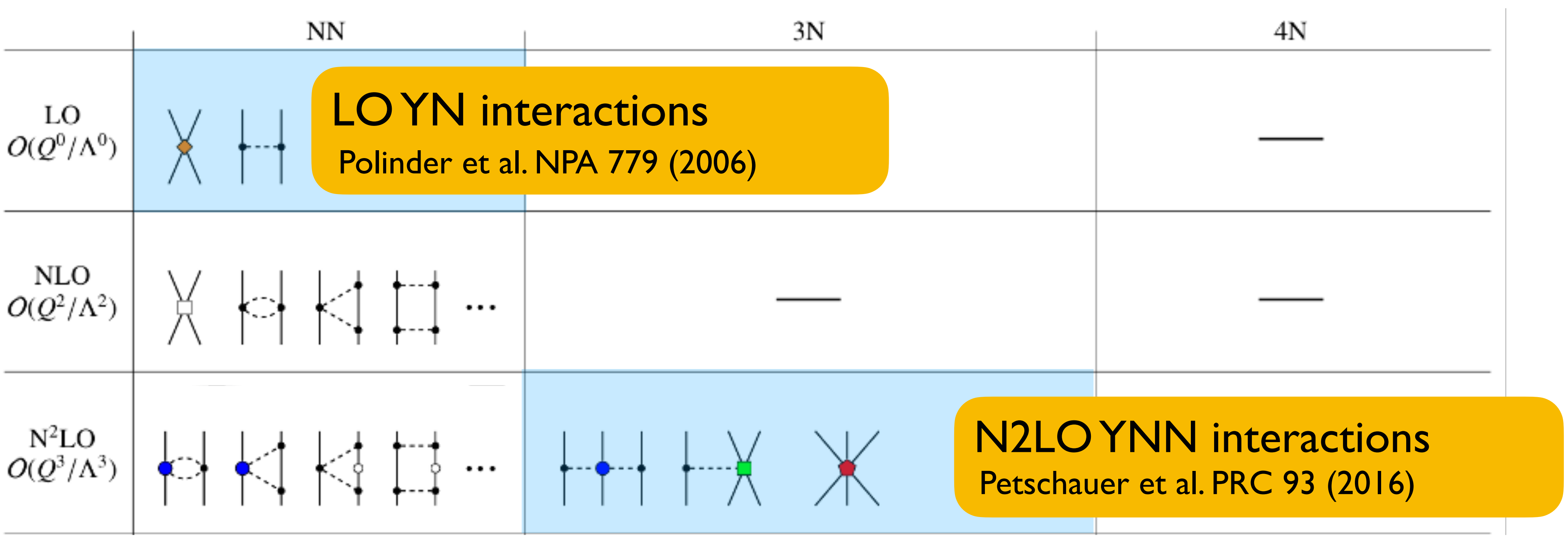

- presently, interactions loosely constrained (only 35 YN scattering data points)
- all interactions are implemented such that all LEC values and regulator functions can be adjusted in an easy and flexible way

Hypermatter: Examples of long-range interactions

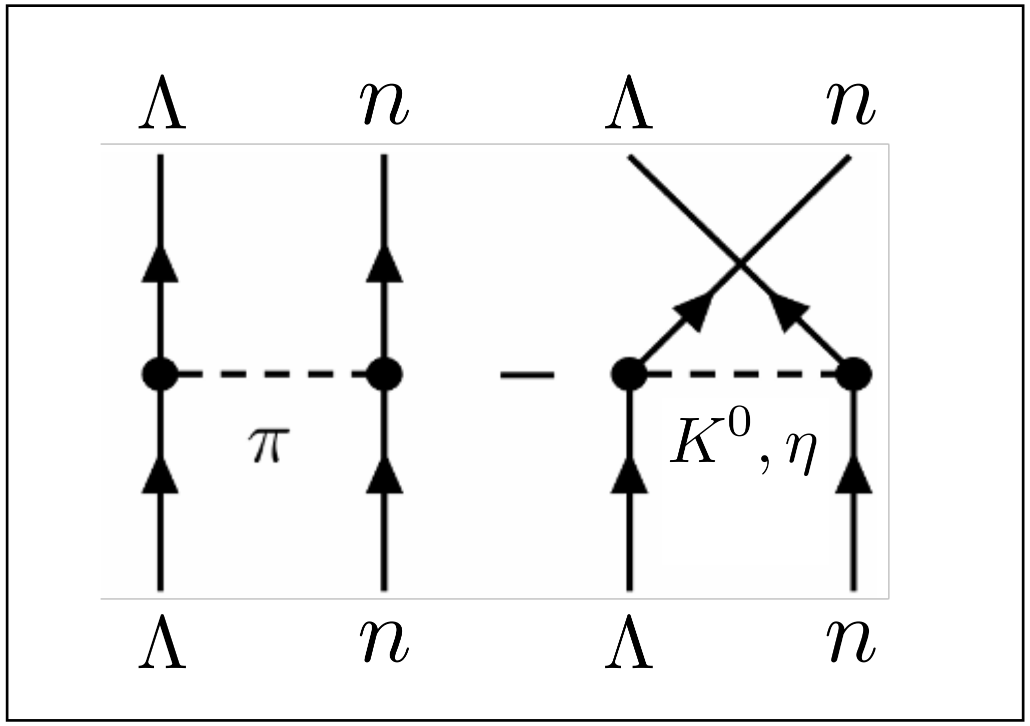

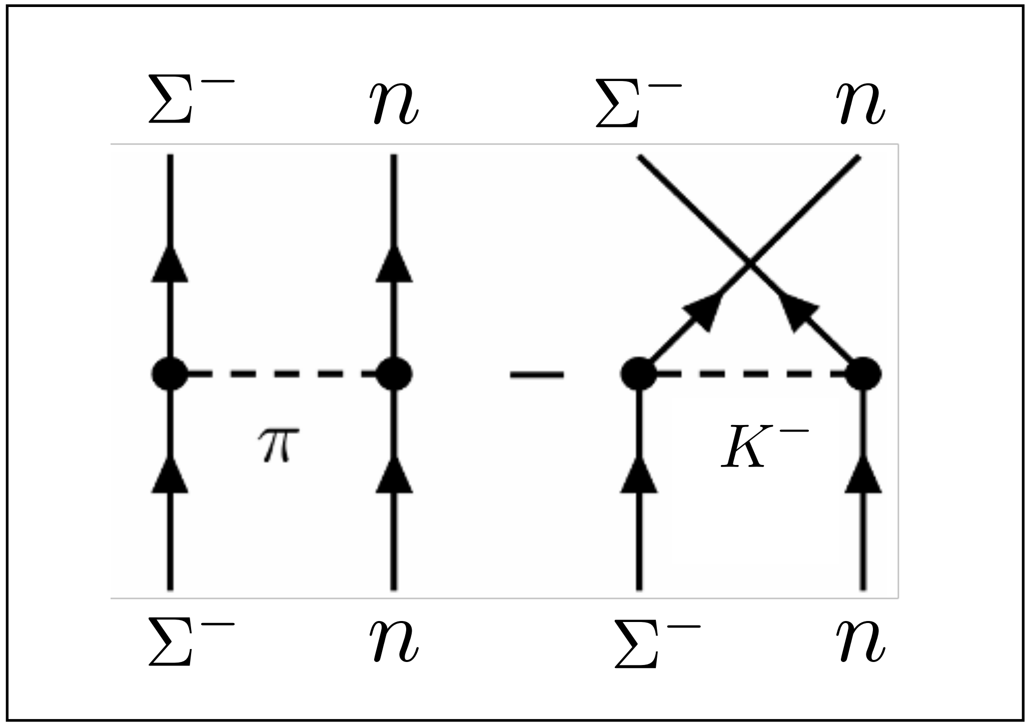

Meson	Symbol	Quark Content	Mass (MeV)
Charged Pion	π^+, π^-	$u\bar{d}$, $d\bar{u}$	139.57
Neutral Pion	π^0	$\frac{1}{\sqrt{2}}(u\bar{u} - d\bar{d})$	134.98
Charged Kaon	K^+, K^-	$u\bar{s}$, $s\bar{u}$	493.68
Neutral Kaon	K^0, $\bar{K}^0$	$d\bar{s}$, $s\bar{d}$	497.61
Eta Meson	η	Mixed state $(u\bar{u}, d\bar{d}, s\bar{s})$	547.86

- Since kaons and eta mesons are much heavier than the pion, "long-range" YN interactions are of short-range nature than NN interactions
- Interactions also allow for flavor-changing processes like

$$\Lambda n \to \Sigma^0 n, \Lambda n \to \Sigma^- p \text{ etc.}$$

Hypermatter:
Many-body calculations

- Goal: Incorporate YN and YNN interactions in existing MBPT framework

- Hartree-Fock:

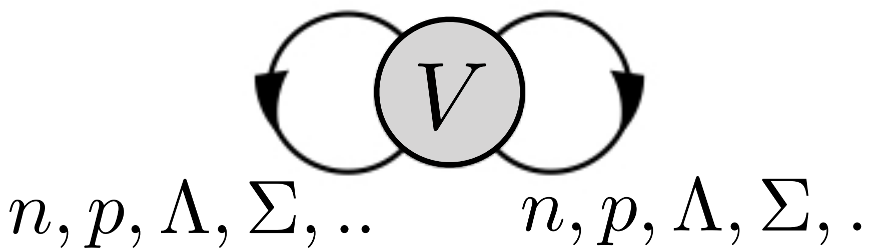

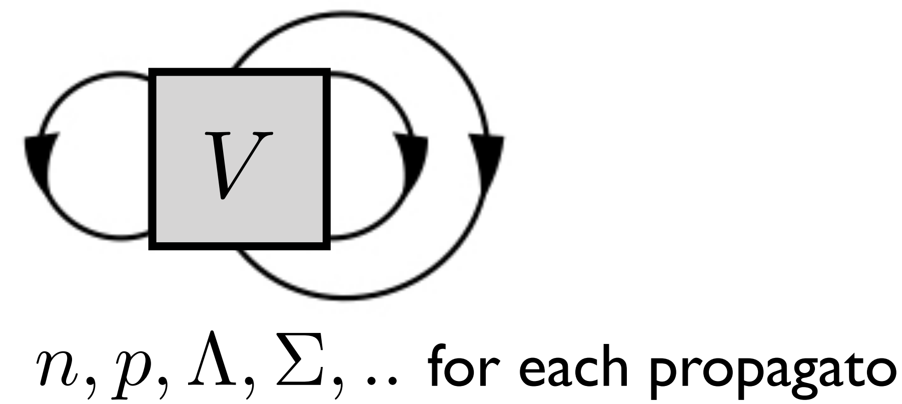

- 2nd-order:
  (example)

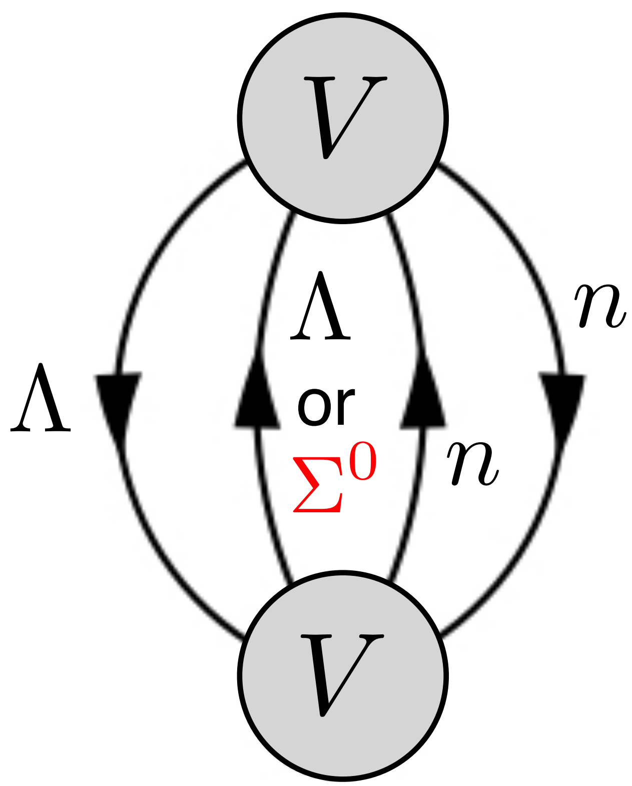

Contributions at 2nd order and higher from flavor-changing particle conversion contributions

Hypermatter: Preliminary results at Hartree-Fock level

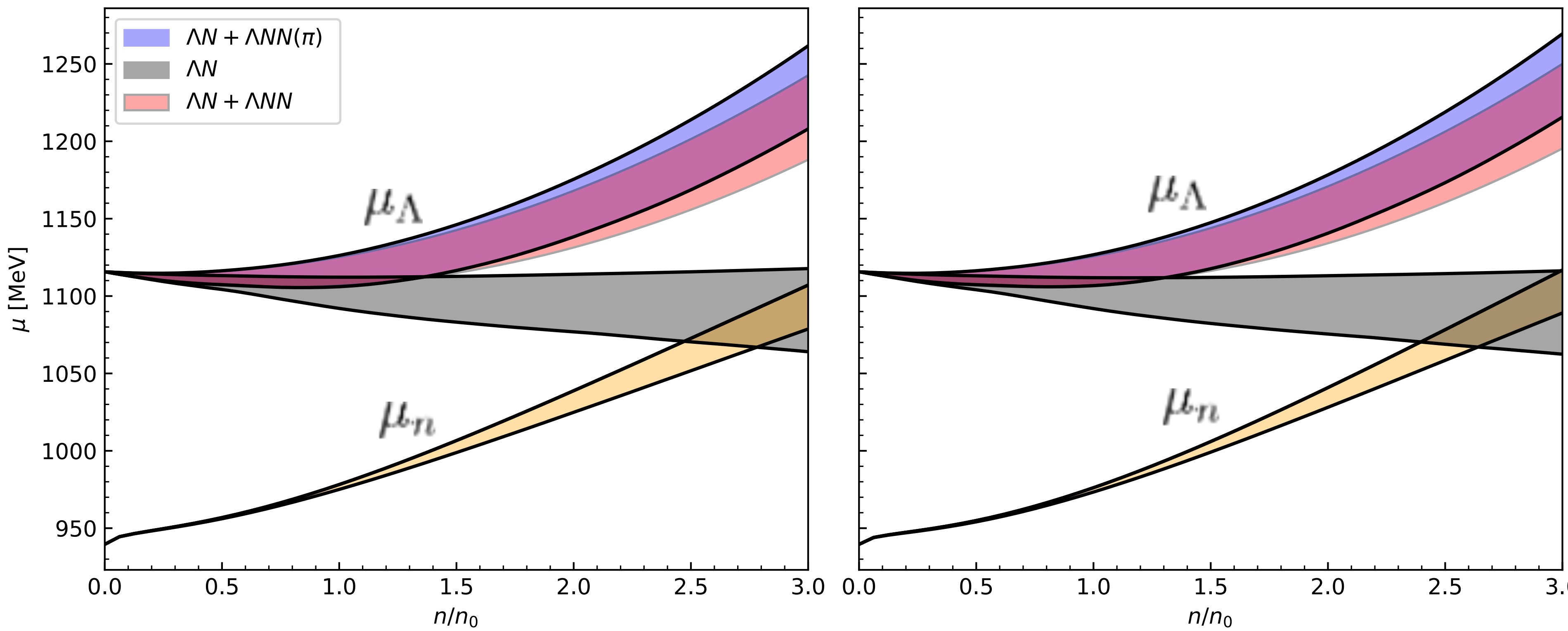

$x = 0.05$ $\qquad$ $x = 0.1$

- Results based on NN+3N interactions using EMN 450/500 MeV
- No hyperons present in system when YNN are included
- We found indications that HF is not a good approximation
- Need to include higher-order contributions in many-body expansion and also in the chiral expansion of YN/YNN interactions

Conclusions

- versatile MBPT framework for nuclear matter at general T that allows to efficiently treat NN and 3N interactions
- phase diagram of nuclear matter in inner crust of NS, phase coexistence and neutron/proton drip
- critical temperature of SNM and asymmetric nuclear matter
- First steps towards extension of MBPT framework to hypermatter, open points:
  - ✦ improved many-body treatment of YN and YNN interactions
  - ✦ improved YN and YNN interactions: extension to higher chiral orders and improved fits of LECs